

Role of ENSO and IOD in the Indian Summer Monsoon Variability: A Review

Pratap Kumar Mohanty and Sanjukta Rani Padhi

Department of Marine Sciences
Berhampur University, Berhampur-760007, Odisha
Email: pratap_mohanty@yahoo.com

ABSTRACT

The Indian Summer Monsoon Rainfall (ISMR) has contributed almost 75.3% to the annual rainfall during 1901-2020 and is considered as the lifeline of India for a sustainable agriculture and economy. ISMR exhibits significant spatial and temporal variability in the form intra-seasonal, seasonal, interannual and biennial oscillations. In the present study, we have used gridded Indian Meteorological Department (IMD) rainfall data from 1901 to 2020 with 0.250x0.250 resolution and have focused on ISMR variability due to coupled ocean atmosphere processes in the Indian and Pacific oceans. As proxies of these coupled ocean atmosphere processes, we consider the role of ENSO and IOD on ISMR. Although several studies were carried out on these aspects during the last two and half decades, the present study is different from other and aims to examine the ISMR variability during 1901-2020 over All India (AI) and different homogeneous zones (NEI, NWI, CI and SPI) under El Nino, La Nina, +ve and -ve IOD (without any co-occurrence) and with co-occurrence of El Nino with +ve IOD and La Nina with -ve IOD. Considering the changing relationship of ISMR with ENSO and IOD, this study also focuses on regional ISMR variability due to various ENSO-IOD conditions.

Keywords: ISMR, ENSO, IOD, Homogeneous zones and Precipitation concentration index.

1. Introduction

Agricultural practices in India and in many other south Asian countries are intricately linked to the performance of the monsoon, particularly ISMR (Parthasarathy et al., 1988). Considering significant spatial-temporal variabilities of ISMR forced from both internal and external forcing, understanding ISMR variability and its prediction is extremely important. Since the internal forcing, mainly intra-seasonal oscillations set a limit to the predictability, major focus are on understanding external forcing including the coupled ocean-atmosphere interaction, SST, snow cover etc. to improve prediction of ISMR. Besides other external forcing, the El Nino Southern Oscillation (ENSO) and Indian Ocean Dipole (IOD) are widely considered as the two major climate drivers of ISMR (Ashok et al., 2001; Behera & Ratnam, 2018; Cherchi et al., 2021; Hrudya et al., 2020; Krishnaswamy et al., 2014; Rajeevan & Pai, 2007; Saji et al., 1999; Varikoden et al., 2020; Webster et al., 1999). Past studies have elucidated on the relationship of ISMR with ENSO and IOD. However, weakening relationship between ENSO and ISMR after 1970s was revealed by studies conducted during the last two decades (Ashok et al., 2019; Kawamura et al., 2005; Kumar et al., 1999), which lead to study the

impacts of IOD on ENSO-ISMR relationship (Ashok et al., 2001). The weakening relationship was attributed to shift in the spatial correlation pattern over the Indian subcontinent from northwest to north east. The study revealed that when the ENSO-ISMR correlation is low (high), the IOD-ISMR correlation is high (low). Many other studies (Anil et al., 2016; Ashok et al., 2004; Gadgil et al., 2004; Webster et al., 1999) also indicated that frequent emergence of the IOD have weakened the otherwise robust relationship between ENSO and ISMR. Thus, it was made apparent that IOD, which moderates the meridional circulation by inducing anomalous convergence (divergence) pattern over Bay of Bengal during positive (negative) IOD events, leads to excessive (deficit) monsoon rainfall over the monsoon trough region (Ashok et al., 2003). This feature was evident in the typical IOD year of 1994 (Behera et al., 1999) and positive IOD year 1997. Studies indicated the influences of ENSO and IOD on the ISMR as opposite to one another (Ashok et al., 2004; Ashok & Saji, 2007). Years with co-occurrence of +ve IOD with El Nino (1961, 1963, 1967, 1972, 1977, 1982, 1983, 1994 and 1997) have positive anomalies of rainfall along the monsoon trough area, the west coast and northwest India while in years with pure +ve IOD events

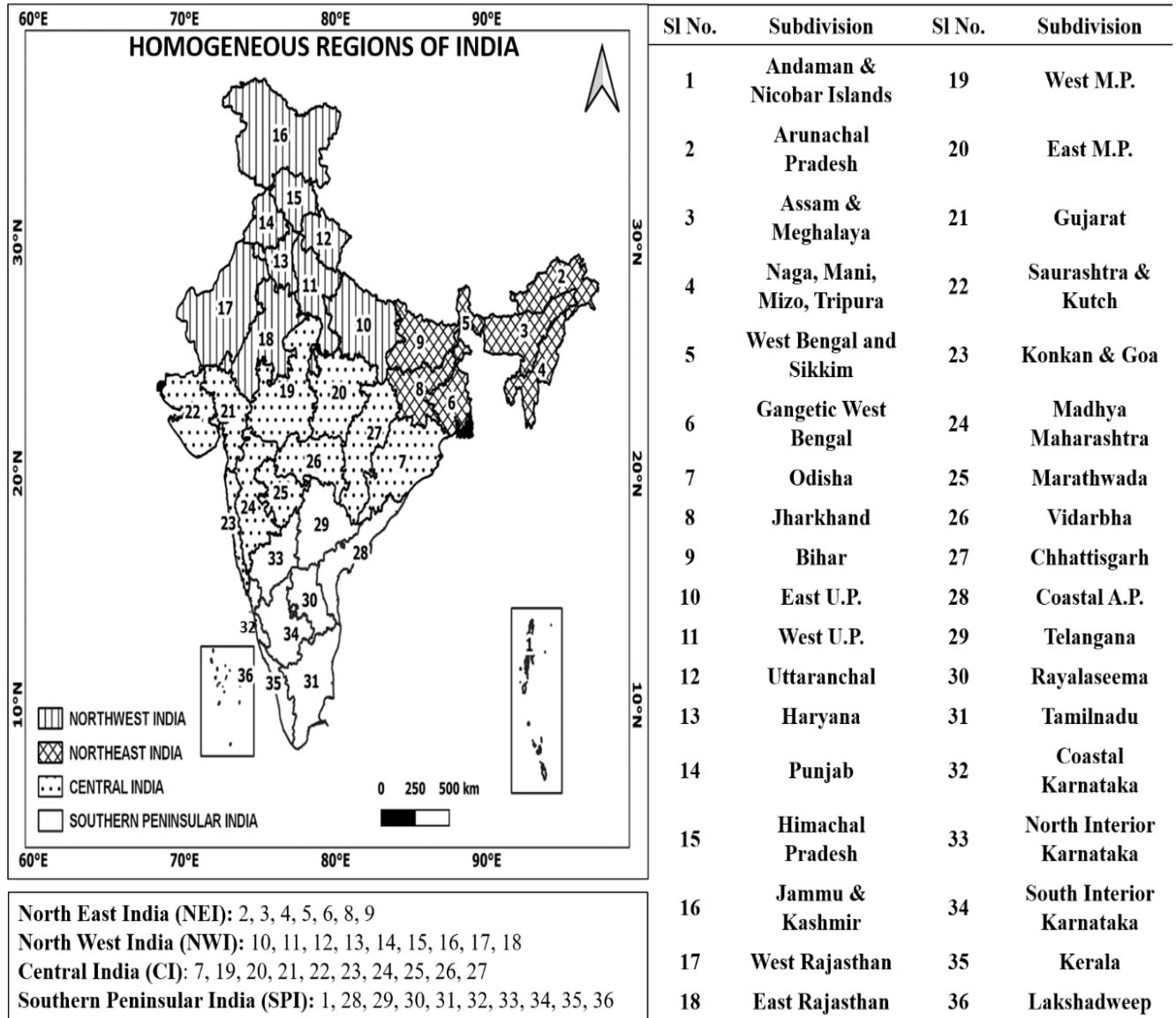


Figure 1: Meteorological subdivisions of India and the four homogeneous zones.

(1961, 1967, 1977 and 1994) significant positive anomalies were found over Indian monsoon trough region, parts of central and southern India and in the regions north of monsoon trough. Differences in rainfall anomaly patterns were also reported during pure La Nina years and years with co-occurrence of La Nina with -ve IOD. Hence, it is apparent that pure El Nino/La Nina, +ve IOD/-ve IOD and their co-occurrences have impacts on ISMR with distinct regional differences, which require detailed investigation. Therefore, in the present study, we focus on the role of ENSO and IOD on ISMR variability over All India (AI) and four homogeneous zones (NEI, NWI, CI and SPI). Figure 1 depicts the constitution of each homogeneous zone in terms of subdivision and the corresponding number.

2. Spatio-temporal Variability of ISMR

ISMR exhibits variability in all time scales as well as in regional scale (Guhathakurta et al., 2015). The regional variations of ISMR are closely related to the variations in the trends of means and extremes of ISMR and were carried out exclusively (Fukushima et al., 2019; Goswami et al., 2006; Guhathakurta et al., 2015; Kothawale & Rajeevan, 2017; Mohapatra, 2018; Oza & Kishtawal, 2014; Rajeevan et al., 2008; Varikoden et al., 2013; Varikoden & Revadekar, 2019). It is not uncommon to find some areas of deficient rain even with best All India (AI) monsoon performance and some areas of excessive rainfall even with the worst AI monsoon performance. Therefore, it is desirable to consider homogeneous zones of Indian monsoon

rainfall and then to find out their association with the regional/global scale circulation features and boundary forcing (Dash et al., 2009; Nair et al., 2018). ISMR does not show any significant trend but there are large variations in regional scale (Guhathakurta & Rajeevan, 2008). While considering 36 meteorological subdivisions of India for the period 1901-2003, Guhathakurta & Rajeevan (2008) showed decreasing trend in rainfall patterns over three subdivisions (Jharkhand, Chhattisgarh and Kerala) and increasing trend over eight subdivisions (Gangetic West Bengal, western Uttar Pradesh, Jammu and Kashmir, Konkan and Goa, Madhya Maharashtra, Rayalaseema, coastal Andhra Pradesh, and north Interior Karnataka). Guhathakurta et al. (2015) analysed ISMR for the period 1901-2011 and observed multidecadal variability in rainfall over four homogeneous zones (NEI, NWI, CI and PI) and found that their phases are different; increasing trend prior to 1950 and decreasing trend in post 1950. Kishore et al. (2015), considered rainfall over West Coast, East Coast, interior peninsula, Northeast, North Central, Northwest and the Western Himalayas and showed incoherent variabilities from region to region. Cash et al. (2015) reported that variations in rainfall over Western Ghats, the Ganges basin, the Bay of Bengal and Bangladesh–NEI are independent of each other as the correlation are not significant. Oza & Kishtawal (2014) analysed the rainfall pattern over different meteorological subdivision of India for the period 1951-2010 and showed a decreasing trend in AI ISMR and a strong decreasing trend in NEI. Konwar et al. (2012) analysed the rainfall trend over western (eastern) parts of India and showed that the trends of low and moderate rainfall events are increasing (decreasing) in recent decades and attributed the increasing trend in the western part to the enhanced vertically integrated moisture transport (VIMT) over the Arabian Sea and decreasing trend in the eastern part to the decreased VIMT over BOB. Zheng et al. (2016) used gridded daily rainfall data for the period 1951-2014 and depicted the daily rainfall behaviour over four homogeneous zones similar to our study (NEI, NWI, CI and SPI) and concluded that rainfall rates are stronger (weaker) over NWI, CI and SPI during strong (weak) monsoons, while rainfall rates over

NEI do not vary much between strong and weak monsoons.

2.1 Spatial variability of ISMR

Climatology (1901-2020) and standard deviation of gridded IMD rainfall over AI and four homogeneous zones (NEI, NWI, CI, and SPI) are depicted in Figure 2(a) and Figure 2(b) respectively. It may be mentioned that subdivision 1 (Andaman and Nicobar Islands) and 36 (Lakshadweep) are not included in the present study due to unavailability of data.

ISMR contributes 75.3% to the annual rainfall over India (1144.4mm). The mean ISMR for AI is 861.64mm having Standard Deviation (SD) 275.45mm and Coefficient of Variation (CV) 32.0%. NEI records the highest ISMR (1366.3mm) as compared to other homogeneous zones. Within NEI, north-central parts of Arunachal Pradesh, parts of West Bengal and Sikkim and south of Assam and Meghalaya record the highest rainfall (>2000mm) as well as highest SD (>750mm). ISMR climatology within NEI is lowest in most parts of Bihar (<1000mm) except eastern Bihar. Within NEI, ISMR has lowest SD over Jharkhand and Western Gangetic West Bengal.

ISMR climatology is lowest (541.48mm) over NWI as compared to other homogeneous zones, while SD is 219.74mm and CV is 40.58% (highest among homogeneous zones). Within NWI, western parts of Himachal Pradesh, south-west parts of Uttaranchal and eastern part of East U.P record relatively higher rainfall (>1000mm) and higher SD (>250mm) in all the three subdivisions. In rest of the subdivisions within NWI, ISMR is less than 1000mm and SD is less than 250mm. CI has ISMR climatology of 987.31mm with SD of 279mm and CV is 28.25%. Within CI, Konkan and Goa records highest rainfall (>2000mm) followed by Odisha, Chhattisgarh and East M.P (1000-2000mm), ISMR in other subdivisions is less than 1000mm. SD is highest (>750mm) in Konkan and Goa followed by other subdivisions except Marathwada and Madhya Maharashtra (lowest SD; >250mm).

ISMR climatology in SPI is 657.7mm with SD of 216mm and CV is 32.84%. Within SPI, Coastal

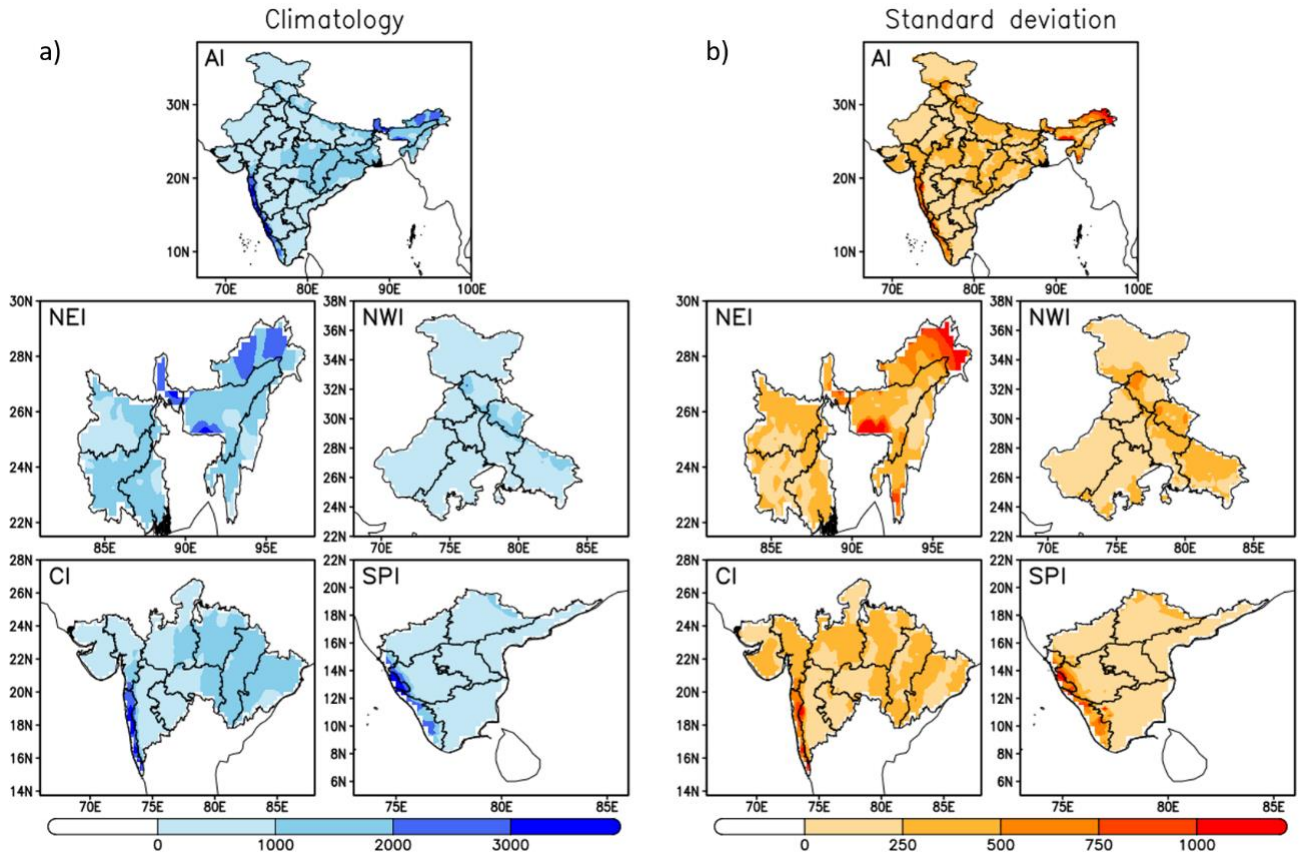


Figure 2: Climatology and standard deviation (1901-2020) of rainfall (mm/year) for AI and four homogeneous zones during Summer monsoon (JJAS).

Karnataka and Kerala have ISMR >2000mm while other subdivisions have ISMR <1000mm. SD trend of SPI is similar to ISMR climatology with highest value of >500mm. Other subdivisions within SPI have SD less than 250mm.

2.2 Temporal variability of ISMR

Temporal variations (1901-2020) of ISMR in AI and the four homogeneous zones are depicted in Figure 3. AI, CI and SPI show a minor increasing trend while NWI and NEI show decreasing trend. But what is distinct from one homogeneous zone to the other is the variability in magnitude of mean annual ISMR and the corresponding trend lines. AI trend line oscillates between 665-1025mm, while in NEI, the oscillation of trend line is at a higher level (1078-1824mm). Trend line oscillates between 702-1320mm, in CI, between 395-890mm in SPI and between 306-825mm in NWI. NWI and NEI mostly covers the monsoon trough region and the decreasing trend in ISMR points to the possibility of shift of monsoon trough towards south giving rise an increasing trend in CI and SPI.

2.3 Precipitation distribution pattern

Precipitation Concentration Index (PCI) was computed following Kumar & Jaswal, (2014) and Oliver, (1980) to understand the precipitation of distribution pattern over AI and the four homogeneous zones. Out of the four categories (Figure 4), PCI shows three categories of distribution; Uniform distribution ($PCI \leq 10$) over NEI, major parts Odisha and north-eastern parts of coastal Andhra Pradesh and Telangana, moderate distribution ($11 \leq PCI \leq 15$) over Bihar, major subdivisions of NWI, CI and SPI and Irregular precipitation ($16 \leq PCI < 20$) over West Rajasthan, Saurashtra & Kutch and a small area over Jammu and Kashmir and Tamilnadu. Temporal variation in PCI shows uniformly distributed precipitation over NEI during 1901-2020. CI show temporal trend mostly limited to Moderate type except a few years (1906, 1910, 1917, 1933, 1934, 1936, 1945, 1970, 1975 and 1998) having Uniform distribution. Temporal trend in SPI is mostly of moderate type except 2010 and 2020 having uniform distribution. Temporal trend in NWI show a relatively greater

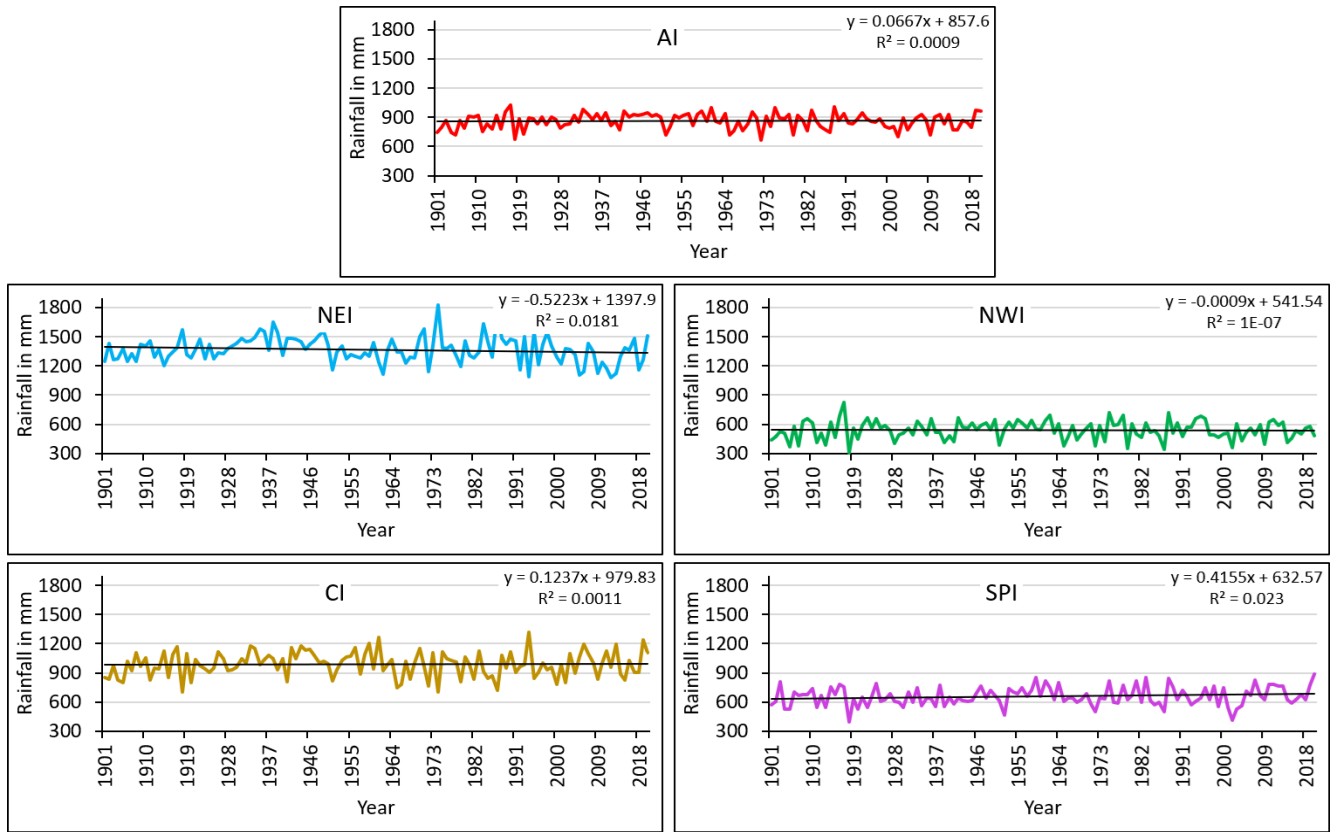


Figure 3: Temporal variation of ISMR for the period 1901-2020.

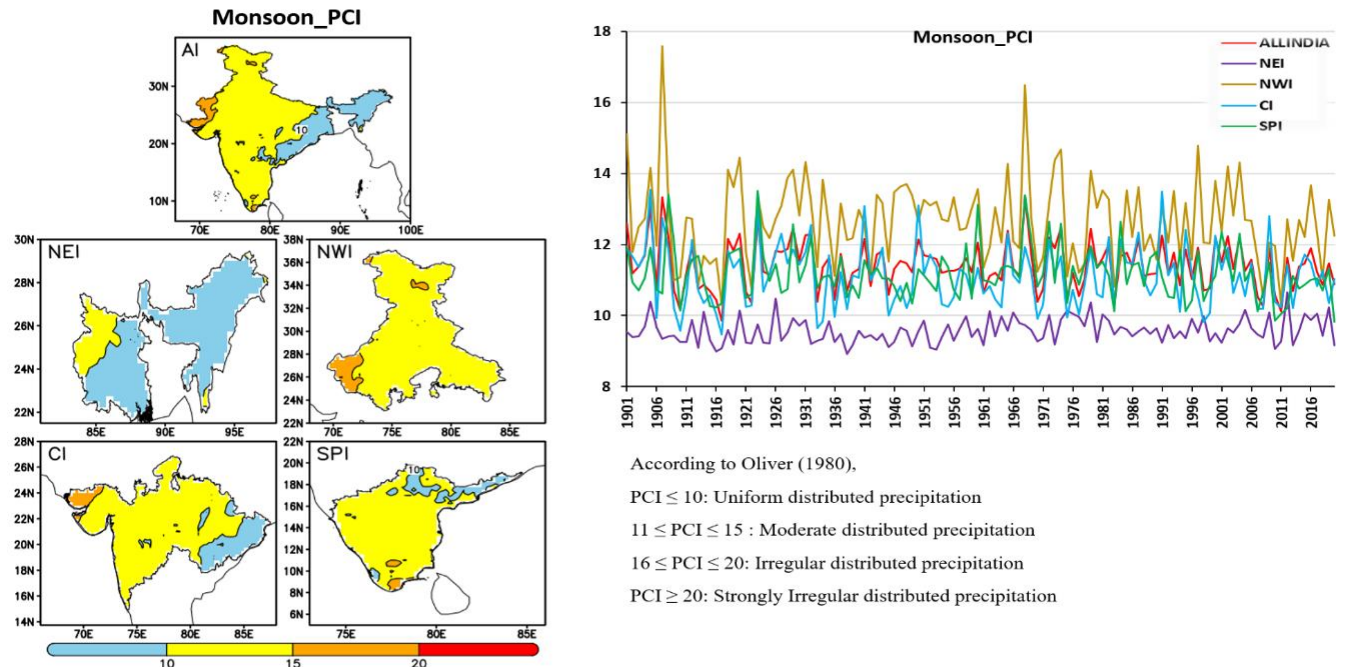


Figure 4: Precipitation Concentration Index (PCI) for AI and four homogeneous zones during Summer monsoon (JJAS).

variability as compared to other homogeneous zones. PCI trends in NWI shows two years with irregular distribution (1907 and 1968) and moderated distribution in rest of the years.

3. ENSO and ISMR Variability

The ENSO has been considered as the most important external forcing of ISMR, until a dipole

mode, IOD was discovered in the Indian Ocean (Saji et al., 1999; Webster et al., 1999). Several studies reported the link of ENSO with ISMR variability. In the first half of the 20th century, six El Nino events were accompanied by severe Indian Monsoon failure. Modulation of the Indian Monsoon by El Nino depends on the location of maximum warming in the equatorial Pacific (Krishna Kumar et al., 2005). Studies indicated ISMR variability associated with both wind and SST anomalies in the Indo-Pacific sector. The indirect relationship between monsoon and El Nino involve circulation anomalies which develop in response to the principal diabatic heating anomalies and SST patterns in the west Pacific, which are themselves a remote response to El Nino (Slingo & Annamalai, 2000). Their study indicated that ISMR anomalies are the consequence of a subtle balance between the suppressing effects of the Walker circulation and the enhancing effects of the local Hadley circulation. The interdecadal variation of ISMR is strongly correlated with the interdecadal variations of various indices of ENSO.

Pacific SST and the Indian monsoon are linked through an interaction between the regional monsoon Hadley circulation and the equatorial Walker circulation, whether it is on the interdecadal or the interannual timescale. Significant surface wind anomalies in the active regions of central and eastern equatorial Pacific associated with strong (weak) ISM are essentially due to the SST anomalies associated with El Nino and La Nina (Goswami & Jayavelu, 2001). The link between ENSO and the Indian Ocean is quite robust in the seasonal scale. Krishnamurthy & Kirtman (2003) found strong correlation of the Indian Ocean SST mode events (considered independently) and the combined variability of the Indian and Pacific Oceans with the ENSO variability. Their study indicated that when strong (weak) monsoon and La Nina (El Nino) coincide the effect of the Indian monsoon is enhanced and the lagged relation between the monsoon and ENSO is mediated through the air–sea interactions in the Indian Ocean. Pacific SST and the Indian monsoon are linked through an interaction between the regional monsoon Hadley circulation and the equatorial

Walker circulation, whether it is on the interdecadal or the interannual timescales (Krishnamurthy & Goswami, 2000). Out of phase (a warm ENSO is correlated with a dry monsoon) suggest that coupled processes in the Pacific and Indian Oceans play distinctly different role in terms of the Indian monsoon–ENSO relationship. Relationship was revealed (Wu & Kirtman, 2004) through coupled model study. However, the study also revealed an in-phase relationship when the Indian Ocean is decoupled and climatological mean SST from the coupled model is used to force the atmosphere in the Indian Ocean sector. Annamalai & Liu (2005) elucidated the relative and combined roles of remote (Pacific) and local (Indian Ocean) forcing in ISM variability. The teleconnection from the main El Nino warm anomalies in the equatorial central eastern Pacific, and the regional circulation anomalies forced by the cold SST anomalies over the equatorial west Pacific and eastern Indian Ocean, play a role in the ENSO–monsoon linkage. A study using long data records (1881–1998) demonstrated that atmospheric conditions over the Indian Ocean help explain the relationship between ENSO and ISMR (Ihara et al., 2007). Reduction (increase) in length of the rainy season and monsoon rainfall was observed due to El Nino (La Nina) forced late (early) onset and early(late) withdrawal (Xavier et al., 2007). The strength of ENSO-ISM relationship shows considerable decadal fluctuations, which have been previously linked to low-frequency climatic processes such as shifts in ENSO's center of action (Yun & Timmermann, 2018). Anomalously warm conditions during boreal summer over the eastern tropical Pacific, result in anomalously deficit rainfall over India during summer monsoon season. Ashok et al. (2019) observed association of El Nino (La Nina) events with a weaker than normal (greater than normal rainfall) summer monsoon rainfall over India. Impacts of El Nino on ISMR variability at homogeneous zone level were limited. Ashok et al. (2004) showed that due to the modulation of the Walker circulation, strong anomalous low-level divergence causes the deficit rainfall over the Indian region during the summers of pure El Nino years (1965, 1969, 1976, 1986, 1987, and 1991) and most of the Indian peninsula

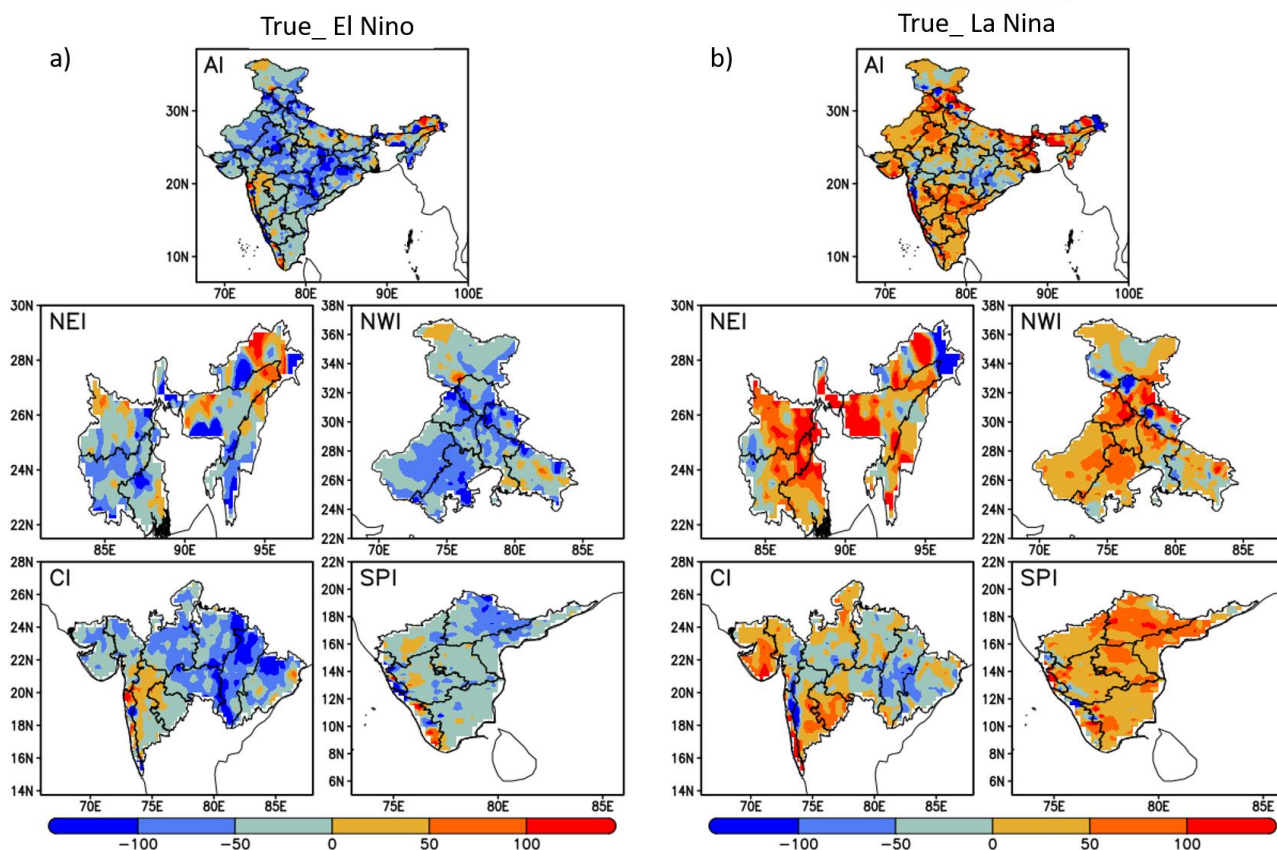


Figure 5: Composite rainfall anomaly (mm) in true El Nino and La Nina years.

and monsoon trough regions receive surplus rainfall anomalies during pure La Nina years (1967, 1973, 1975, 1988, and 1999). Guhathakurta et al. (2015) used monthly rainfall data of IMD from 2001-2011 and showed the existence of multidecadal variability of four homogeneous regions of India having different phases. The study showed that only rainfall of Peninsular India has positive correlation with El Nino years while other three homogeneous regions (NWI, CI, NEI) as well as all-India rainfall have strong negative correlations. Considering very limited study on the regional ISMR variability vis-à-vis ENSO/IOD, the present study uses a long period recent gridded rainfall data (1901- 2020) at higher resolution ($0.25^0 \times 0.25^0$) and provides a details association between ISMR of four homogeneous zone and ENSO/IOD (individual events) and their co-occurrences.

Majority of the pure El Nino events are associated with significant reduction in monsoon rainfall and widespread drought conditions due to anomalous subsidence over the Indian subcontinent, associated with changes in the zonal walker circulation and

weakening of the onshore monsoon circulation over India.

3.1 True El Nino/La Nina and ISMR

Composite rainfall anomaly for AI and four homogeneous zones (NEI, NWI, CI and SPI) during true El Nino years (Figure 5a) and true La Nina years (Figure 5b) are prepared using IMD gridded rainfall data from 1901-2020. These 120 years period was categorised as El Nino (La Nina) years based on Nino 3.4 index (1901-1949) and ONI data (1950-2020) following <https://climatedataguide.ucar.edu/climate-data/nino-sst-indices-nino-12-3-34-4-oni-and-tni>. Years were identified as El Nino (La Nina) when Nino 3.4 SST exceeded $+0.4^0\text{C}$ (-0.4^0C) for six consecutive months and more, and if ONI SST exceeded $+0.5^0\text{C}$ (-0.5^0C) for five consecutive months and more. True El Nino (La Nina) years were identified when only El Nino (La Nina) event occurred and there were no co-occurrences with IOD.

During true El Nino (La Nina) years, predominance of negative (positive) rainfall anomalies are

Table 1. Positive and negative anomalies over AI and its different homogeneous zones during different composite years.

| Composite | Region | % of positive anomaly | % of negative anomaly |
|----------------------------------|---------------|------------------------------|------------------------------|
| True_El Nino | AI | 14.2 | 85.8 |
| | NEI | 25.1 | 74.9 |
| | NWI | 10.0 | 90.0 |
| | CI | 12.4 | 87.6 |
| | SPI | 13.3 | 86.7 |
| True_La Nina | AI | 70.1 | 29.9 |
| | NEI | 73.2 | 26.8 |
| | NWI | 75.4 | 24.6 |
| | CI | 50.7 | 49.3 |
| | SPI | 90.7 | 9.3 |
| True_Positive_IOD | AI | 64.9 | 35.1 |
| | NEI | 29.1 | 70.9 |
| | NWI | 76.7 | 23.3 |
| | CI | 75.6 | 24.4 |
| | SPI | 55.1 | 44.9 |
| True_Negative_IOD | AI | 62.1 | 37.9 |
| | NEI | 33.6 | 66.4 |
| | NWI | 65.0 | 35.0 |
| | CI | 62.3 | 37.7 |
| | SPI | 87.7 | 12.3 |
| El Nino with Positive_IOD | AI | 23.7 | 76.3 |
| | NEI | 36.6 | 63.4 |
| | NWI | 22.1 | 77.9 |
| | CI | 13.6 | 86.4 |
| | SPI | 31.5 | 68.5 |
| La Nina with Negative_IOD | AI | 83.7 | 16.3 |
| | NEI | 72.3 | 27.7 |
| | NWI | 78.9 | 21.1 |
| | CI | 93.9 | 6.1 |
| | SPI | 89.9 | 10.1 |

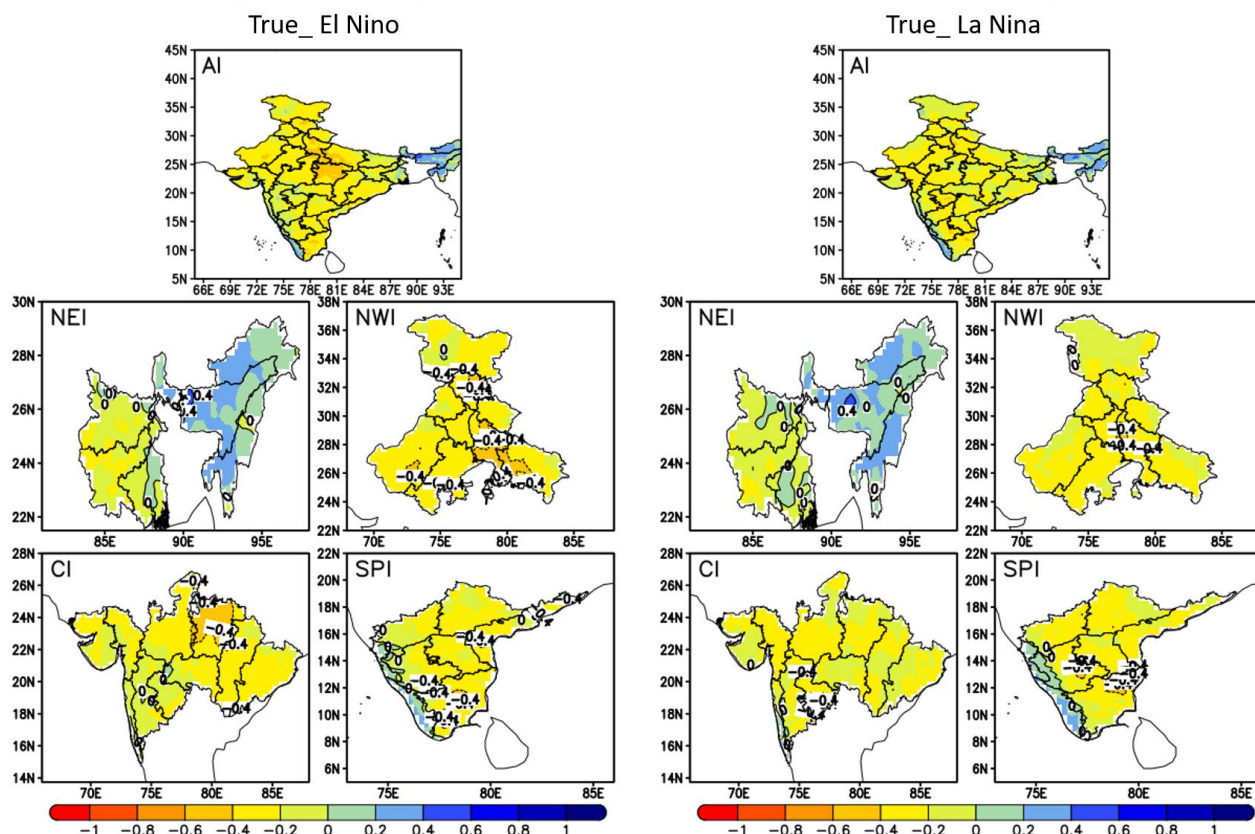


Figure 6: Correlation between ISMR and Nino 3.4 index for true El Nino and La Nina years.

distinctly evident over AI and over other homogeneous zones. AI positive rainfall anomaly during El Nino (La Nina) was 14.2% (70.1%), while negative rainfall anomaly during El Nino (La Nina) was 85.8% (29.9%)(Table 1). The results are in agreement with Guhathakurta et al. (2015); Hrudya et al. (2020); Pandey et al. (2015); Varikoden et al. (2020). Over NEI, positive rainfall anomaly during true El Nino (La Nina) was 25.1% (73.2%) while negative rainfall anomaly during true El Nino (La Nina) was 74.9% (26.8%).

However, during El Nino (La Nina) years, rainfall anomalies over Arunachal Pradesh, Assam and Meghalaya and Western Bihar were positive (negative). NWI recorded 10% (90%) lowest (highest) positive (negative) rainfall anomaly during true El Nino years. On the other hand, during true La Nina years positive (negative) rainfall anomaly was 75.4% (24.6%). Positive (negative) rainfall anomaly trend during La Nina (El Nino) is not reflected over north of Jammu and Kashmir. Over CI, positive rainfall anomaly during true El Nino (La Nina) years was 12.4% (50.7%) while negative rainfall anomaly was 87.6%

(49.3%). It is evident that over CI, positive rainfall anomaly during La Nina years is lowest as compared to other homogeneous zones. Therefore, rainfall anomalies over central Odisha, Chhattisgarh, east M.P are negative even during La Nina years. Over SPI, positive rainfall anomaly during true El Nino (La Nina) years was 13.3% (90.7%), while negative rainfall anomaly was 86.7% (9.3%). The rainfall anomaly trend indicates that SPI records highest (lowest) positive (negative) rainfall anomaly during La Nina years. The rainfall anomaly trend during true El Nino years is opposite to that during true La Nina years except over southern Kerala.

3.2 Relationship between Nino 3.4 SST and ISMR

Figure 6 depicts spatial correlation between ISMR and Nino 3.4 SST during true El Nino and La Nina years for AI as well as for four homogeneous zones. In agreement with earlier studies (Ashok & Saji, 2007; Hrudya et al., 2021) true El Nino events reduce the ISMR over India. However, Ashok & Saji (2007) showed correlation between Nino 3

index and ISMR. Positive and significant correlation (95-99%) between Nino 3.4 SST and ISMR are observed over Assam and Meghalaya, southern part of Arunachal Pradesh, Mizoram, Tripura and Kerala.

The correlation between Nino 3.4 and ISMR is negative and significant at 99% over East M.P, central Tamilnadu, east and west U.P, while 95% significance level with negative correlation are over rest of the subdivisions. During true La Nina years, area of positive correlation between Nino 3.4 SST and ISMR reduces compared to during true El Nino years. For example, correlations are not significant over Meghalaya and Mizoram during true La Nina years while there is slight enhanced correlation over Kerala. Significance level of negative correlation during true La Nina years reduces as compared to during true El Nino years.

4. IOD and ISMR Variability

There have been many studies on IOD-ISMIR relationship during the last two decades since the seminal work by Saji et al., (1999) showing a dipole mode in the Indian Ocean. IOD is independent of the ENSO in the Pacific Ocean. Their study revealed that during a dipole mode event rainfall decreases over the oceanic tropical convergence zone and increases over the western tropical Indian ocean. Also, the impact of monsoonal circulation on dipole mode was revealed. However, statistical correlation of the DMI with precipitation over the Asian monsoon region did not yield any significant relationship. Hence the relationship between ISMR and DMI remained unexplained. Later Ashok et al. (2001) studied the impact of IOD on the relationship between ISMR and ENSO and showed that when the ENSO-ISMIR correlation is low (high), the IOD-ISMIR correlation is high (low). While trying to answer whether the moving correlation between the IOD-ISMIR changes from decade to decade, and its role in the weakening of the monsoon-ENSO correlation, their study demonstrated that IOD events affect ISMR on their own and apparently weaken or strengthen the influence of ENSO on the ISMR. In an AGCM ensemble simulation study (Li et al., 2003), it was revealed that a positive phase of IODM enhance the south Asian monsoon, while the strengthened

monsoon damp the IODM. Individual and combined influences of ENSO and IOD on ISMR (Ashok et al., 2004) were examined, which revealed that positive (negative) IOD significantly reduces the impact of the El Nino (La Nina) on the Indian monsoon and suggested that IODMI can be used as a potential predictor of the Indian monsoon rainfall. Later, Ashok & Saji (2007) studied the impacts of ENSO and IOD on sub-regional ISMR and showed that the ENSO (IOD) index is negatively (positively) correlated with summer monsoon rainfall over seven (four) of the eight homogeneous rainfall zones over India. Relationship between IOD and ISMR was studied (Bala & Singh, 2008) using data from 1960-2002 and it was revealed that stronger/weaker western pole during April-May is associated with delayed/early monsoon onset over Kerala and the study showed a good relationship between IODM and ISMR over PI during withdrawal phase of the monsoon. Influence of ENSO and IOD on ISMR was studied by Cherchi & Navarra (2013), and it was revealed that the relationship between ENSO, IOD and ISMR is not constant in time and ISMR in El Nino/La Nina years or in +ve/-ve IOD events are not exactly symmetric. In agreement with Saji et al.(1999), Krishnaswamy et al.(2014) showed that IOD evolves independent of ENSO. Whether spatially explicit ENSO and IOD for larger regions can be mapped to identify vulnerable and sensitive areas is not known. Anil et al. (2016) examined the role of early IOD (EIOD), normal IOD and prolonged IOD (PIOD) on ISMR and showed that EIOD and PIOD significantly enhance ISMR under moderate DMI. ISMR correlation with ENSO and IOD was assessed using Climate models (Li et al., 2017) and it was revealed that there is an overly strong IOD-ISMIR negative correlation in the present day simulation, suggesting that positive IOD tend to reduce ISMR. Behera & Ratnam (2018) assessed the quasi-asymmetric response of the ISMR in relation to IOD and showed that CI and monsoon trough region, have asymmetric response with above normal rainfall in both phases of IOD and attributed the asymmetric response south and east of monsoon trough region to the nature of teleconnection and moisture distributions over India during positive/negative IOD. Changes in

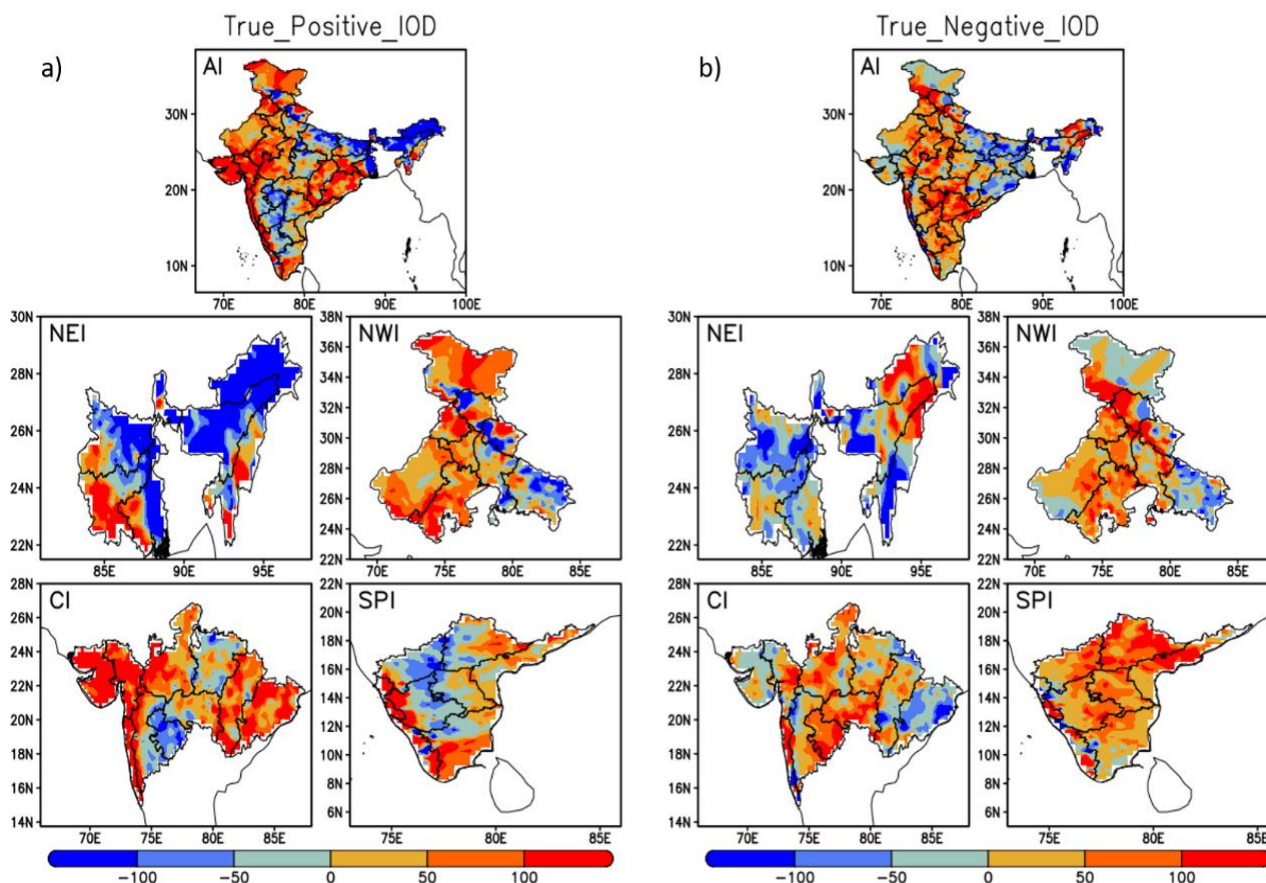


Figure 7: Composite rainfall anomaly (mm) in true positive and negative IOD years.

IOD-ISMR relationship from early 1951-1980 to 1986-2015 was explored (Hrudya et al., 2020) during onset, peak and withdrawal phases of the ISM. The study revealed that IOD-ISMR relationships are strengthening (weakening) during withdrawal (onset) phases over most of the Indian regions during recent decades while during peak phase the relationship changes from out of phase (-ve correlation) to in-phase (+ve correlation) in most parts of India. Their study also showed that during +ve IOD events, increase in rainfall occurs during all phases and in case of -ve IOD, weakening of rainfall occurs during peak and withdrawal phase and increase in onset phase.

From the above literature review it is apparent that ENSO-IOD-ISMR relationship is changing with time. ENSO-IOD relationship with ISMR has also significant spatial variability, which is least explored. Therefore, in the present study we try to explore the ENSO-IOD impacts individually as well during their co-occurrence on ISMR of AI and different homogeneous zones (NEI, NWI, CI and SPI).

The intensity of the IOD is commonly measured by an index that is anomalous SST gradient between the Western Equatorial Indian Ocean (WEIO) (50°E–70°E and 10°S–10°N) and the South-Eastern Equatorial Indian Ocean (SEEIO) (90°E–110°E and 10°S–0°) region (Saji et al., 1999). The index is called the DMI. When the DMI is positive, then the phenomenon is referred to as the +ve IOD, and when it is negative, it is referred to as -ve IOD (Meyers et al., 2007). The index was standardized by the standard deviation to give them equal weight in the classification method. In this study, we have computed the mean of the DMI from June to November of every year and standardized it, and assigned the value to represent the DMI of that particular year. Then, the mean and standard deviation [SD (σ)] of standardized DMI for the climatology period (1901-2020) have been computed. We categorized the year as positive (+ve) IOD if the mean standardized DMI (June–November) is greater than or equal to mean+1SD and as negative (-ve) IOD if the mean standardized DMI (June–November) is less than or equal to mean-1SD (Mahala et al., 2015).

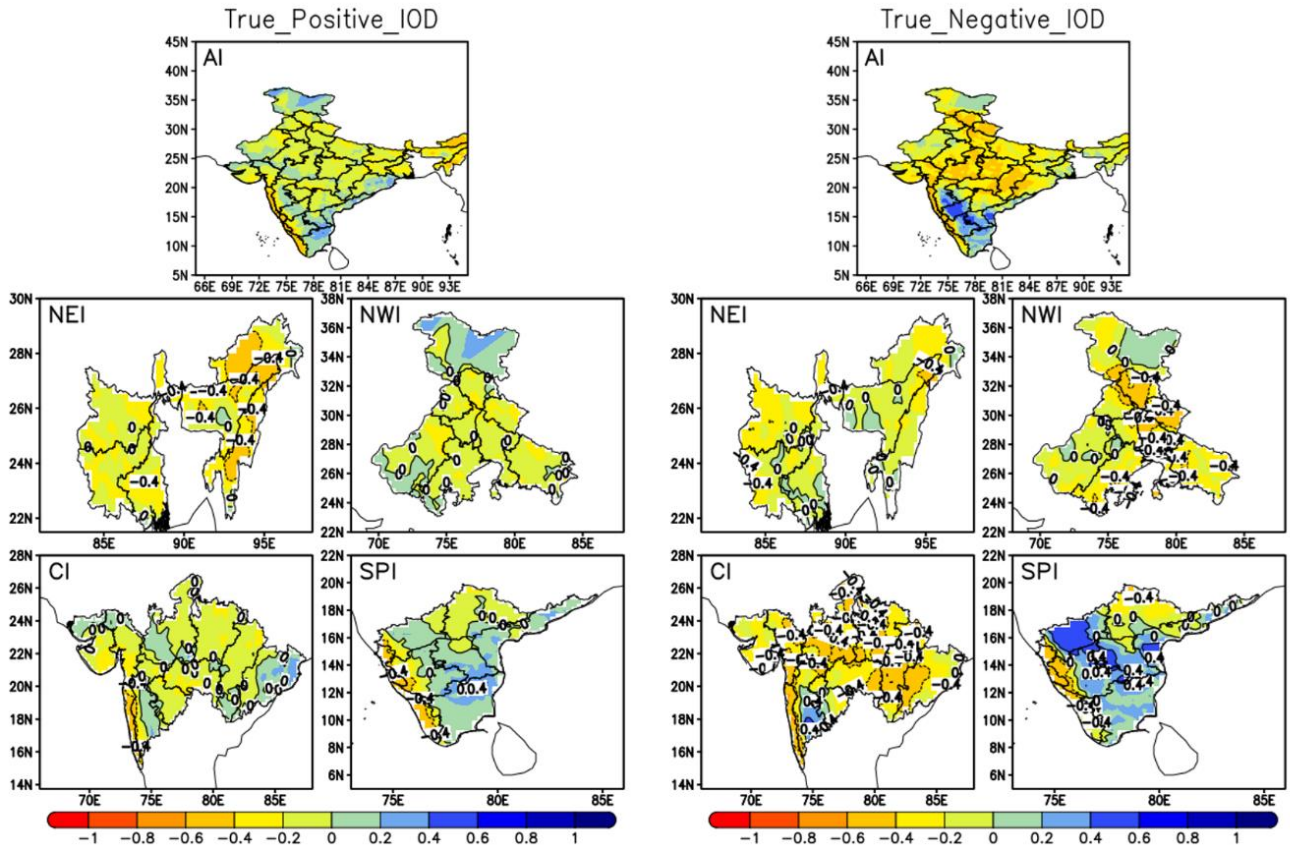


Figure 8: Correlation between ISMR and SST (WEIO-SEEIO) for true positive and negative IOD years.

4.1 True +ve/-ve IOD and ISMR

Figure 7 depicts the rainfall distribution over AI and different homogeneous zone during true +ve and -ve IOD years. During the study periods (1901-2020), 12 years are identified as true +ve IOD and 10 years as true -ve IOD. 1992 is not considered as true -ve IOD year as it was an year of cooccurrence with El Nino year. True +ve IOD events are associated with surplus rainfall anomalies over India (Ashok & Saji, 2007). The study showed positive correlation between Indian Ocean Dipole Mode Index (IODMI) and ISMR over monsoon trough and north-west region. The present study shows distinctly +ve anomaly over most part of NWI, CI, Jharkhand, western part of Gangetic West Bengal, Coastal Karnataka, Kerala, Tamilnadu, parts of Andhra Pradesh and Telangana. Negative rainfall anomaly during true +ve IOD years are distinct over most parts of NEI (except over Jharkhand, Gangetic West Bengal and Bihar), parts of NWI (East U.P, Uttaranchal, Himanchal Pradesh), parts of SPI (North and South Interior Karnataka) and parts of CI (Marathwada, Madya Maharashtra, East M.P).

During true +ve IOD years, percentage of positive rainfall anomaly (64.9%) is more than negative rainfall anomaly (35.1%) over AI. Percentage distribution of positive rainfall anomaly is highest in NWI (76.7%) followed by CI (75.6%) and SPI (55.1%) and lowest over NEI (29.1%). On the other hand, during true -ve IOD years, percentage of +ve (-ve) anomaly slightly reduces (enhances) over AI (Table 1). Percentage of area with positive anomaly is highest over SPI followed by NWI, CI and NEI (Table 1). Area with negative anomaly during true -ve IOD years is highest over NEI followed by CI, NWI and lowest over SPI.

4.2 Relationship between IODMI and ISMR

Fig 8 depicts a spatial correlation between IODMI and ISMR during true +ve and -ve IOD years over AI and four homogeneous zones. From the correlation distribution it is apparent that both true +ve and -ve IOD years have mostly negative correlation with ISMR over most parts of India except over SPI. Correlation is significant at 90% level over SPI (most part of North and South Interior Karnataka and parts of Andhra Pradesh)

and parts of CI (southern part of Madhya Maharashtra). Significant (90%) and negative correlations over parts of NEI (Arunachala Pradesh, east part of Assam, Mizoram) are observed during true +ve IOD years, while significant (90%) and negative correlations are mostly observed over CI (except Madhya Maharashtra, Marathwada), parts of NWI (Himachal Pradesh, Uttaranchal and West U.P) and parts of SPI (Coastal Karnataka).

Our results clearly suggest that true ENSO (IOD) are not negatively (positively) correlated with ISMR and it is in contrast to some of the earlier studies suggesting that the ENSO (IOD) index is negatively (positively) correlated with ISMR (Ashok & Saji, 2007; Hrudya et al., 2021). Our results are in agreement with Bala & Singh (2008), who indicated that -ve phase of IODMI during March and April is associated with enhance summer monsoon rainfall over peninsular India.

5. Co-occurrence of ENSO, IOD and ISMR Variability

Studies earlier indicated that El Nino condition suppresses the monsoon rainfall over India while +ve phase of IOD is favourable for monsoon rainfall (Ashok et al., 2001; Saji et al., 1999; Webster et al., 1999). However, during co-occurrence of +ve IOD events with El Nino, an anomalous divergent centre is introduced in the eastern tropical Indian ocean. The anomalous divergent flow from this centre crosses the equator and leads to convergence over the Indian monsoon region, while weakening the El Nino induced divergence in the western Pacific. As a result, ENSO induced subsidence is reduced and the rainfall over the eastern flank of the Indian monsoon trough region is enhanced. Over the western part of tropical Indian ocean, anomalous ascending motion over the warm pole during +ve IOD event subside the north of the equator, moves northward, ascend and causes surplus rainfall. As a result, ENSO induced rainfall deficit over Western India and western part of monsoon trough also reduces. Ashok et al. (2004), examined the relative influences of ENSO and IOD on the ISMR and showed that the during the co-occurrence period the low-level divergence over western Pacific, which occurs during true El Nino, is weakened and a new

anomalous divergent centre relative to the true El Nino year is induced off the west coast of Indonesia. As a result, an anomalous weaker circulation over the IOD region is formed. Intensification of cross equatorial Hadley circulation occurs resulting in surplus ISMR. Thus, the +ve IOD events reduce the ENSO influence. Behera et al. (2006) through their Coupled General Circulation Model (CGCM) study indicated that about 29% of IOD events co-evolve with ENSO. Ummenhofer et al. (2011) showed that for El Nino events which co-occur with +ve IOD, Indian Ocean conditions act to counter the El Nino rainfall deficit by enhancing the moisture convergence over Indian subcontinent resulting in surplus monsoon rainfall. When +ve IOD and El Nino co-occur, the SST anomalies in the Indo-Pacific sector and 200mb velocity potential anomalies over India are larger than in the true cases (Cherchi & Navarra, 2013), and as a result monsoon anomalies are almost uniform during La Nina with -ve IOD, while a dipole in the anomalies are evident during El Nino and +ve IOD. Saji & Yamagata (2003) used observational data (1958-1977) and reported that ENSO events co-occurring with IOD events are much stronger compared to non-occurring events. The evolution of the asymmetric pattern in rainfall and surface wind during true El Nino/IOD and co-occurrence years is examined using reanalysis data from 1871-2008 and the study revealed that spring asymmetric mode is well developed due to meridional gradient in SST and SLP when El Nino co-occurred with +ve IOD (Chakravorty et al., 2013).

5.1 Co-occurrence of El Nino with +ve IOD

Figure 9 (a) depicts the rainfall anomaly over AI and four homogeneous zones when El Nino co-occur with +ve IOD (8 events). Under this condition, area of positive (negative) rainfall anomaly over AI was 23.7% (76.3%). During the co-occurrence years, area with positive (negative) anomaly was lowest (highest) over CI followed by NWI (Table 1).

However, parts of Odisha in CI, Jammu and Kashmir in NWI experienced positive rainfall anomaly. Area with percentage of positive anomaly is highest over NEI (36.6%) followed by

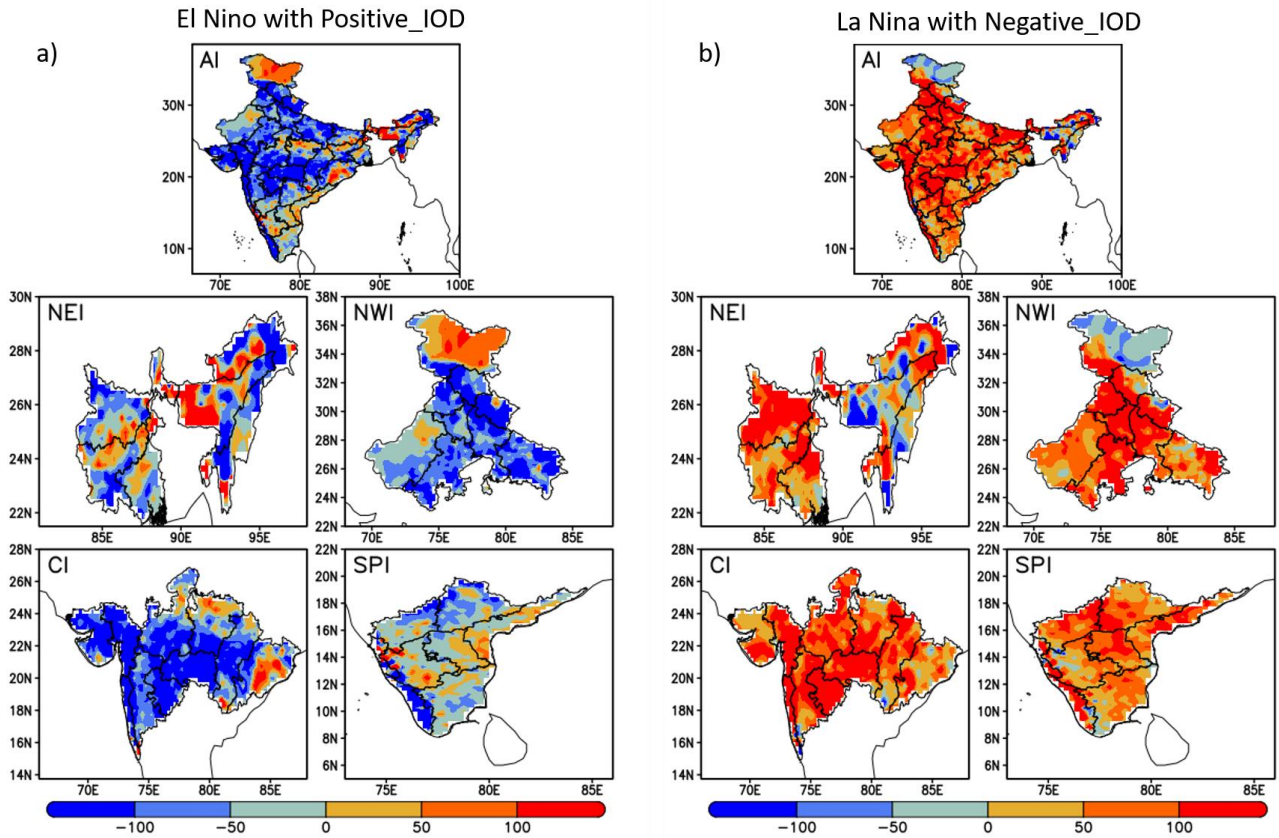


Figure 9: Composite rainfall anomaly (mm) during co-occurrence of El Niño with positive IOD and La Niña with negative IOD.

SPI (31.5%). Our results having 8 co-occurring events (1901-2020), are not in agreement with Ashok, et al. (2004), who used data from 1958-1997 and showed 9 co-occurring events with positive anomalies of rainfall along the monsoon trough area, west coast of India, northwest of India. Parts of NEI such as West Bengal and Sikkim, some parts of Bihar, Jharkhand, Assam & Meghalaya, Tripura and Mizoram experienced positive rainfall anomalies. Similarly in SPI, coastal Andhra Pradesh, some part of South Interior Karnataka and some part of Telangana experience positive rainfall anomaly.

5.2 Co-occurrence of La Niña with -ve IOD

Figure 9 (b) depicts the rainfall anomaly over AI and four homogeneous zones when La Niña co-occurs with -ve IOD (8 events). Area with percentage of positive rainfall anomaly over AI (83.7%) is highest during co-occurrence events compared to true La Niña and true +ve and true -ve IOD events. In the Homogeneous zones, area with percentage of positive (negative) rainfall anomaly is

highest(lowest) over CI followed by SPI, NWI and NEI (Table 1). Parts of NWI (Jammu and Kashmir) and NEI (Mizoram, Manipur and Meghalaya) experienced negative rainfall anomaly. When La Niña co-occurs with -ve IOD the low level western Pacific convergence centre and low level eastern Indian convergence centre are strengthened and a new relatively larger area of convergence covering eastern Indian and western Pacific regions significantly enhances the convection over the region, relative to true La Niña/ -ve IOD events. This creates a strong rising branch of the Walker circulation over the eastern Indian and western Pacific sector and help in expanding the area of Walker circulation over Indian region. As a result, this subsiding branch of the Walker cell during the co-occurrence shifts further west of Indian Ocean relative to normal Walker circulation. Anomalously strong Walker circulation over the eastern Indian and western Pacific leads to intensification of local Hadley cell resulting in anomalous surplus ISMR as in the years of excess AI ISMR (1916, 1933 & 1956) (Figure 10).

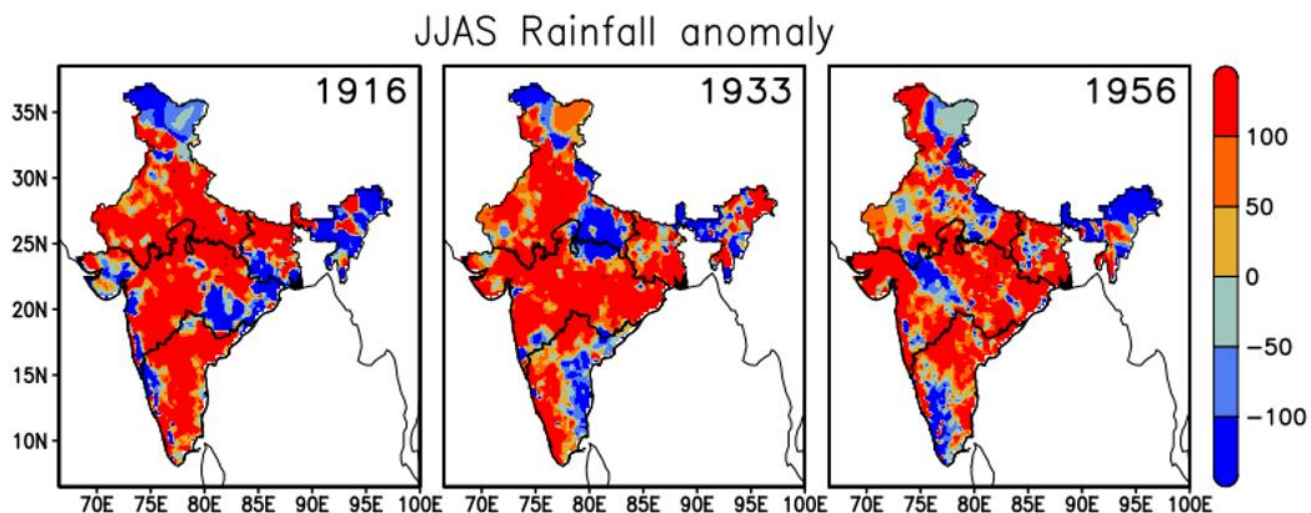


Figure 10: Summer monsoon rainfall (mm) anomaly for 1916, 1933 and 1956.

6. Conclusions

In the present study, an extensive review has been made on the studies focusing on ENSO-IOD-ISMR relationship during the last two and half decade. Our review suggests that there have been many studies on ENSO-ISMR and IOD-ISMR, and a few studies on ENSO-IOD-ISMR, but mostly at AI level. However, impacts of true El Nino/La Nina, +ve IOD/-ve IOD and co-occurrence of El Nino with +ve IOD and La Nina with -ve IOD on ISMR, both at AI and at homogeneous zones and at further regional levels, are not addressed properly leading to a gap in our understanding of ENSO-IOD-ISMR variability. Therefore, in the present study, besides making an extensive review, we also used IMD gridded rainfall data ($0.25^0 \times 0.25^0$) from 1901 to 2020, Nino 3.4 Index (1901-1949) (<https://climatedataguide.ucar.edu/climate-data/nino-sst-indices-nino-12-3-34-4-oni-and-tni>) and ONI data (1950-2020) (<https://climatedataguide.ucar.edu/climate-data/nino-sst-indices-nino-12-3-34-4-oni-and-tni>) and DMI data from 1901-2020 (<https://psl.noaa.gov/data/timeseries/DMI>) and examined the ISMR variability over AI and four homogeneous zone (NEI, NWI, CI and SPI) under true El Nino/La Nina, true +ve/-ve IOD and co-occurrence of El Nino with -ve IOD and La Nina with -ve IOD.

Study on spatial variability of ISMR indicates 75.3% contribution of ISMR to the annual rainfall over India (1144.4mm). NEI records the highest

ISMR (1366.3mm) as compared to other homogeneous zones. ISMR climatology is lowest (541.48mm) over NWI as compared to other homogeneous zones and CV is 40.58% (highest among homogeneous zones). CI has ISMR climatology of 987.3mm and within CI, Konkan and Goa record highest rainfall (> 2000mm). ISMR climatology in SPI is 657.7mm, and within SPI, Coastal Karnataka, and Kerala have ISMR > 2000mm. North-central parts of Arunachal Pradesh, parts of West Bengal and Sikkim, and south of Assam and Meghalaya also record the highest rainfall (>2000mm). Temporal variability in ISMR indicates minor increasing trend in AI, CI, and SPI while NWI and NEI show a decreasing trend. Uniform distribution ($PCI \leq 10$) over NEI, major parts of Odisha and north-eastern parts of coastal Andhra Pradesh and Telangana, moderate distribution ($11 \leq PCI \leq 15$) over Bihar, major subdivisions of NWI, CI, and SPI, and Irregular precipitation ($16 \leq PCI < 20$) over West Rajasthan, Saurashtra & Kutch and a small area over Jammu and Kashmir and Tamil Nādu are observed from the variation in PCI.

During true El Nino (La Nina) years, predominance of negative (positive) rainfall anomalies are distinctly evident over AI and other homogeneous zones. NWI recorded lowest positive (10%) and highest negative (90%) rainfall anomaly during true El Nino years while during true La Nina years positive(negative) rainfall anomaly was 75.4% (24.6%). Over CI, positive rainfall anomaly during true El Nino (La Nina) years was 12.4% (50.7%)

while negative rainfall anomaly was 87.6% (49.3%). However, positive rainfall anomaly during La Nina years is lowest in CI as compared to other homogeneous zones. The rainfall anomaly trend indicates that SPI records the highest (lowest) positive (negative) rainfall anomaly during the La Nina years while the trend is opposite during true El Nino years except over southern Kerala. In agreement with earlier studies, we found that true El Nino events reduce the ISMR over India. During true La Nina years, the area of positive correlation between Nino 3.4 SST and ISMR reduce as compared to during true El Nino years. The significance level of negative correlation during true La Nina years reduces as compared to during true El Nino years.

During true +ve IOD years percentage of positive rainfall anomaly (64.9%) is more than negative rainfall anomaly (35.1%) over AI. Percentage distribution of positive rainfall anomaly is highest in NWI (76.7%) followed by CI (75.6%) and SPI (55.1%) and lowest over NEI (29.1%). On the other hand, during true -ve IOD years percentage of +ve (-ve) anomaly slightly reduces (enhances) over AI. Percentage of area with positive anomaly is highest over SPI followed by NWI, CI and NEI. Area with negative anomaly during true -ve IOD years is highest over NEI followed by CI, NWI and lowest over SPI. On the other hand, during true -ve IOD years, percentage of +ve (-ve) anomaly slightly reduces (enhances) over AI. Both true +ve and -ve IOD years have mostly negative correlation (significant at 90%) with ISMR over most parts of India except over SPI.

When El Nino co-occurred with +ve IOD events, areas of positive and negative rainfall anomalies over AI were 23.7% and 76.3% respectively. During the co-occurrence years, area with positive (negative) anomaly was lowest (highest) over CI followed by NWI. However, the area with a percentage of positive anomaly is highest over NEI (36.6%) followed by SPI (31.5%). Area with the percentage of positive rainfall anomaly over AI (83.7%) is highest during co-occurrence of La Nina and -ve IOD events compared to true La Nina and true +ve and true -ve IOD events. In the homogeneous zones, area with a percentage of

positive (negative) rainfall anomaly is highest (lowest) over CI followed by SPI, NWI and NEI when La Nina co-occurred with -ve IOD events.

Acknowledgements

One of the authors (SRP) acknowledges the financial support from DST, Government of India for offering INSPIRE Fellowship. Authors also acknowledge the help and support provided by Berhampur University.

References

- Anil, N., Ramesh Kumar, M. R., Sajeev, R., & Saji, P. K. (2016). Role of distinct flavours of IOD events on Indian summer monsoon. *Natural Hazards*, 82(2), 1317–1326. <https://doi.org/10.1007/s11069-016-2245-9>
- Annamalai, H., & Liu, P. (2005). Response of the Asian summer monsoon to changes in El Niño properties. *Quarterly Journal of the Royal Meteorological Society*, 131(607), 805–831. <https://doi.org/10.1256/qj.04.08>
- Ashok, K., Chan, W. Le, Motoi, T., & Yamagata, T. (2004). Decadal variability of the Indian Ocean dipole. *Geophysical Research Letters*, 31(24), 1–4. <https://doi.org/10.1029/2004GL021345>
- Ashok, K., Feba, F., & Tejavath, C. T. (2019). The Indian summer monsoon rainfall and ENSO. *Mausam*, 70(3), 443–452
- Ashok, K., Guan, Z., Saji, N. H., & Yamagata, T. (2004). Individual and combined influences of ENSO and the Indian Ocean Dipole on the Indian summer monsoon. *Journal of Climate*, 17(16), 3141–3155. [https://doi.org/10.1175/1520-0442\(2004\)017<3141:IACIOE>2.0.CO;2](https://doi.org/10.1175/1520-0442(2004)017<3141:IACIOE>2.0.CO;2)
- Ashok, K., Guan, Z., & Yamagata, T. (2001). Impact of the Indian Ocean dipole on the relationship between the Indian monsoon rainfall and ENSO. *Geophysical Research Letters*, 28(23), 4499–4502. <https://doi.org/10.1029/2001GL013294>
- Ashok, K., Guan, Z., & Yamagata, T. (2003). A look at the relationship between the ENSO and the Indian Ocean Dipole. *Journal of the Meteorological Society of Japan*, 81(1), 41–56. <https://doi.org/10.2151/jmsj.81.41>

- Ashok, K., & Saji, N. H. (2007). On the impacts of ENSO and Indian Ocean dipole events on sub-regional Indian summer monsoon rainfall. *Natural Hazards*, 42(2), 273–285. <https://doi.org/10.1007/s11069-006-9091-0>
- Bala, I., & Singh, O. P. (2008). Relationship between Indian ocean dipole mode and summer monsoon. *Mausam*, 59(2), 167–172.
- Behera, S. K., Krishnan, R., & Yamagata, T. (1999). Unusual ocean-atmosphere conditions in the tropical Indian Ocean during 1994. *Geophysical Research Letters*, 26(19), 3001–3004. <https://doi.org/10.1029/1999GL010434>.
- Behera, Swadhin K., Luo, J. J., Masson, S., Rao, S. A., Sakuma, H., & Yamagata, T. (2006). A CGCM study on the interaction between IOD and ENSO. *Journal of Climate*, 19(9), 1688–1705. <https://doi.org/10.1175/JCLI3797.1>.
- Behera, Swadhin K., & Ratnam, J. V. (2018). Quasi-asymmetric response of the Indian summer monsoon rainfall to opposite phases of the IOD. *Scientific Reports*, 8(1), 1–8. <https://doi.org/10.1038/s41598-017-18396-6>.
- Cash, B. A., Kinter, J. L., Adams, J., Altshuler, E., Huang, B., Jin, E. K., Manganello, J., Marx, L., & Jung, T. (2015). Regional structure of the Indian summer monsoon in observations, reanalysis, and simulation. *Journal of Climate*, 28(5), 1824–1841. <https://doi.org/10.1175/JCLI-D-14-00292.1>.
- Chakravorty, S., Chowdary, J. S., & Gnanaseelan, C. (2013). Spring asymmetric mode in the tropical Indian Ocean: Role of El Niño and IOD. *Climate Dynamics*, 40(5–6), 1467–1481. <https://doi.org/10.1007/s00382-012-1340-1>
- Cherchi, A., & Navarra, A. (2013). Influence of ENSO and of the Indian Ocean Dipole on the Indian summer monsoon variability. *Climate Dynamics*, 41(1), 81–103. <https://doi.org/10.1007/s00382-012-1602-y>
- Cherchi, A., Terray, P., Ratna, S. B., Sankar, S., Sooraj, K. P., & Behera, S. (2021). Indian Ocean Dipole influence on Indian summer monsoon and ENSO: A review. In *Indian Summer Monsoon Variability* (pp. 157–182). Elsevier. <https://doi.org/10.1016/b978-0-12-822402-1.00011-9>
- Dash, S. K., Kulkarni, M. A., Mohanty, U. C., & Prasad, K. (2009). Changes in the characteristics of rain events in India. *Journal of Geophysical Research*. <https://doi.org/10.1029/2008JD010572>.
- Fukushima, A., Kanamori, H., & Matsumoto, J. (2019). Regionality of long-term trends and interannual variation of seasonal precipitation over India. *Progress in Earth and Planetary Science*, 6(1), 1–20.
- Gadgil, S., Vinayachandran, P. N., Francis, P. A., & Gadgil, S. (2004). Extremes of the Indian summer monsoon rainfall, ENSO and equatorial Indian Ocean oscillation. *Geophysical Research Letters*, 31(12). <https://doi.org/10.1029/2004GL019733>.
- Goswami, B. N., & Jayavelu, V. (2001). On possible impact of the Indian summer monsoon on the ENSO. *Geophysical Research Letters*, 28(4), 571–574. <https://doi.org/10.1029/2000GL011485>.
- Goswami, B. N., Venugopal, V., Sengupta, D., Madhusoodanan, P., & Xavier, P. K. (2006). Increasing trend of Extreme Rain Events Over India in a Warming Environment. *Research and Exploration*, December, 1442–1445.
- Guhathakurta, P., & Rajeevan, M. (2008). Trends in the rainfall pattern over India. *International Journal of Climatology*, 28(11), 1453–1469. <https://doi.org/10.1002/joc.1640>.
- Guhathakurta, P., Rajeevan, M., Sikka, D. R., & Tyagi, A. (2015). Observed changes in southwest monsoon rainfall over India during 1901–2011. *International Journal of Climatology*, 35(8), 1881–1898. <https://doi.org/10.1002/joc.4095>.
- Hrudya, P. H., Varikoden, H., & Vishnu, R. (2021). A review on the Indian summer monsoon rainfall, variability and its association with ENSO and IOD. In *Meteorology and Atmospheric Physics* (Vol. 133, Issue 1). Springer Vienna. <https://doi.org/10.1007/s00703-020-00734-5>.
- Hrudya, P. P. V. H., Varikoden, H., & Vishnu, R. N. (2021). Changes in the relationship between Indian Ocean dipole and Indian summer monsoon

- rainfall in early and recent multidecadal epochs during different phases of monsoon. *International Journal of Climatology*, 41(S1), E305–E318. <https://doi.org/10.1002/joc.6685>
- Ihara, C., Kushnir, Y., Cane, M. A., & Pena, V. H. D. (2007). The impact of the positive Indian Ocean dipole on Zimbabwe droughts Tropical climate is understood to be dominated by. *International Journal of Climatology*, 2029, 179–187. <https://doi.org/10.1002/joc>
- Kawamura, R., Uemura, K., & Suppiah, R. (2005). On the Recent Change of the Indian Summer Monsoon-ENSO Relationship. *Sola*, 1, 201–204. <https://doi.org/10.2151/sola.2005-052>
- Kishore, P., Jyothi, S., Basha, G., Rao, S. V. B., Rajeevan, M., Velicogna, I., & Sutterley, T. C. (2015). Precipitation climatology over India: validation with observations and reanalysis datasets and spatial trends. *Climate Dynamics*, 46(1–2), 541–556. <https://doi.org/10.1007/s00382-015-2597-y>
- Konwar, M., Parekh, A., & Goswami, B. N. (2012). Dynamics of east-west asymmetry of Indian summer monsoon rainfall trends in recent decades. *Geophysical Research Letters*, 39(10), 1–6. <https://doi.org/10.1029/2012GL052018>
- Kothawale, D. R., & Rajeevan, M. (2017). Monthly , Seasonal and Annual Rainfall Time Series for All-India , Homogeneous Regions and Meteorological Subdivisions : 1871-2016. Indian Institute of Tropical Meteorology (IITM) Earth System Science Organization, Ministry of Earth Sciences, 02, 1–164.
- Krishna Kumar, K., Hoerling, M., & Rajagopalan, B. (2005). Advancing dynamical prediction of Indian monsoon rainfall. *Geophysical Research Letters*, 32(8), 1–4. <https://doi.org/10.1029/2004GL021979>.
- Krishnamurthi, V., & Goswami, B. N. (2000). Indian Monsoon ENSO relationship on interdecadal timescale. *American Meteorological Society*, 579–595.
- Krishnamurthy, V., & Kirtman, B. P. (2003). Variability of the Indian Ocean: Relation to monsoon and ENSO. *Quarterly Journal of the Royal Meteorological Society*, 129(590 PART A), 1623–1646. <https://doi.org/10.1256/qj.01.166>
- Krishnaswamy, J., Vaidyanathan, S., Rajagopalan, B., Bonell, M., Sankaran, M., Bhalla, R. S., & Badiger, S. (2014). Non-stationary and non-linear influence of ENSO and Indian Ocean Dipole on the variability of Indian monsoon rainfall and extreme rain events. *Climate Dynamics*, 45(1–2), 175–184. <https://doi.org/10.1007/s00382-014-2288-0>
- Kumar, K. K., Rajagopalan, B., & Cane, M. A. (1999). On the weakening relationship between the Indian monsoon and ENSO. *Science*, 284(5423), 2156–2159. <https://doi.org/10.1126/science.284.5423.2156>
- Kumar, N., & Jaswal, A. (2015). Changes rainfall concentration over India 1871 –. In *High-Impact Weather Events over the SAARC Region* (pp. 325–333).
- Li, T., Wang, B., Chang, C. P., & Zhang, Y. (2003). A theory for the Indian Ocean dipole-zonal mode. *Journal of the Atmospheric Sciences*, 60(17), 2119–2135. [https://doi.org/10.1175/1520-0469\(2003\)060<2119:ATFTIO>2.0.CO;2](https://doi.org/10.1175/1520-0469(2003)060<2119:ATFTIO>2.0.CO;2)
- Li, Z., Lin, X., & Cai, W. (2017). Realism of modelled Indian summer monsoon correlation with the tropical Indo-Pacific affects projected monsoon changes. *Scientific Reports*, 7(1), 1–7. <https://doi.org/10.1038/s41598-017-05225-z>
- Mahala, B. K., Nayak, B. K., & Mohanty, P. K. (2015). Impacts of ENSO and IOD on tropical cyclone activity in the Bay of Bengal. *Natural Hazards*, 75(2), 1105–1125. <https://doi.org/10.1007/s11069-014-1360-8>
- Meyers, G., McIntosh, P., Pigot, L., & Pook, M. (2007). The years of El Niño, La Niña and interactions with the tropical Indian Ocean. *Journal of Climate*, 20(13), 2872–2880. <https://doi.org/10.1175/JCLI4152.1>
- Mohapatra, G. N. (2018). Study of Indian Summer Monsoon Rainfall Trend During the Period 1901-2013 through Data Mining. *International Journal for Research in Applied Science and Engineering Technology*, 6(5), 1701–1705.

<https://doi.org/10.22214/ijraset.2018.5278>

Nair, P. J., Chakraborty, A., Varikoden, H., Francis, P. A., & Kuttippurath, J. (2018). The local and global climate forcings induced inhomogeneity of Indian rainfall. *Scientific Reports*, 8(1), 1–13. <https://doi.org/10.1038/s41598-018-24021-x>

Oliver, J. E. (1980). Monthly precipitation distribution: A comparative index. *The Professional Geographer*, 32(3), 300–309. <https://doi.org/10.1111/j.0033-0124.1980.00300.x>

Oza, M., & Kishtawal, C. M. (2014). Spatial analysis of Indian summer monsoon rainfall. *Journal of Geomatics*, 8(1), 40–47. www.wmo.int/pages/themes/climate/climate_data_and_prod

Pandey, D. K., Rai, S., SHAHI, N. K., & Mishra, N. (2015). Seasonal prediction of ISMR and relationship with EL- NINO and IOD in ECMWF system 4 coupled model. *Climate Change*, 923, 447–455.

Parthasarathy, B., Munot, A. A., & Kothawale, D. R. (1988). Regression model for estimation of indian foodgrain production from summer monsoon rainfall. *Agricultural and Forest Meteorology*, 42(2–3), 167–182. [https://doi.org/10.1016/0168-1923\(88\)90075-5](https://doi.org/10.1016/0168-1923(88)90075-5)

Rajeevan, M., Bhate, J., & Jaswal, A. K. (2008). Analysis of variability and trends of extreme rainfall events over India using 104 years of gridded daily rainfall data. *Geophysical Research Letters*, 35(18). <https://doi.org/10.1029/2008GL035143>

Rajeevan, M., & Pai, D. S. (2007). On the El Niño-Indian monsoon predictive relationships. *Geophysical Research Letters*, 34(4). <https://doi.org/10.1029/2006GL028916>

Saji, N. H., Goswami, B. N., Vinayachandran, P. N., & Yamagata, T. (1999). A dipole mode in the tropical Indian ocean. *Nature*, 401(6751), 360–363. <https://doi.org/10.1038/43854>

Saji, N. H., & Yamagata, T. (2003). Possible impacts of Indian Ocean Dipole mode events on global climate. *Climate Research*, 25(2), 151–169.

<https://doi.org/10.3354/cr025151>

Slingo, J. M., & Annamalai, H. (2000). 1997: The El Niño of the century and the response of the Indian summer monsoon. *Monthly Weather Review*, 128(6), 1778–1797. [https://doi.org/10.1175/1520-0493\(2000\)128<1778:TENOOT>2.0.CO;2](https://doi.org/10.1175/1520-0493(2000)128<1778:TENOOT>2.0.CO;2)

Ummenhofer, C. C., Sen Gupta, A., Li, Y., Taschetto, A. S., & England, M. H. (2011). Multi-decadal modulation of the El Niño-Indian monsoon relationship by Indian Ocean variability. *Environmental Research Letters*, 6(3), 34006–34014. <https://doi.org/10.1088/1748-9326/6/3/034006>

Varikoden, H., Hrudya, P. P. V. H., Vishnu, R. N., & Kuttippurath, J. (2021). Changes in the ENSO–ISMR relationship in the historical and future projection periods based on coupled models. *International Journal of Climatology*, 1–21. <https://doi.org/10.1002/joc.7362>

Varikoden, H., Kumar, K. K., & Babu, C. A. (2013). Long term trends of seasonal and monthly rainfall in different intensity ranges over Indian subcontinent. *MAUSAM*, 64(3), 481–488. <https://mausamjournal.imd.gov.in/index.php/MAUSAM/article/view/730>

Varikoden, H., & Revadekar, J. V. (2019). On the extreme rainfall events during the southwest monsoon season in northeast regions of the Indian subcontinent. *Meteorological Applications*, 27(1). <https://doi.org/10.1002/met.1822>

Webster, P. J., Moore, A. M., Loschnigg, J. P., & Leben, R. R. (1999). Coupled ocean-atmosphere dynamics in the Indian Ocean during 1997-98. *Nature*, 401(6751), 356–360. <https://doi.org/10.1038/43848>

Wu, R., & Kirtman, B. P. (2004). Impacts of the Indian Ocean on the Indian Summer Monsoon-ENSO relationship. *Journal of Climate*, 17(15), 3037–3054. [https://doi.org/10.1175/1520-0442\(2004\)017<3037:IOTIOO>2.0.CO;2](https://doi.org/10.1175/1520-0442(2004)017<3037:IOTIOO>2.0.CO;2)

Xavier, P. K., Marzin, C., & Goswami, B. N. (2007). An objective definition of the Indian summer monsoon season and a new perspective on

the ENSO – monsoon relationship. QUARTERLY JOURNAL OF THE ROYAL METEOROLOGICAL SOCIETY, 133(624), 749–764. <https://doi.org/10.1002/qj.45>.

Yun, K.-S., & Timmermann, A. (2018). Decadal Monsoon-ENSO Relationship Reexamined. *Geophysical Research Letters*, 45(4), 2014–2021.

Zheng, Y., Bourassa, M. A., Ali, M. M., & Krishnrmti, T. N. (2016). Distinctive features of rainfall over the Indian homogeneous rainfall regions between strong and weak Indian summer monsoons. *Journal of Geophysical Research:Atmospheres*, 121(10), 5631–5647.